



Starch based nanocomposites as sensors for heavy metals – detection of Cu²⁺ and Pb²⁺ ions

Gohar Khachatryan * and Karen Khachatryan 

Institute of Chemistry, Faculty of Food Technology, University of Agriculture, 122 Balicka Street, 30-149 Cracow, Poland

Received May 9, 2018; accepted August 22, 2018

Abstract. Inorganic nanocomposites can find application in various branches of industry, including food technology. Quantum dots have already been reported as promising nanosensors for the detection of heavy metal ions in soil, water and food. This study presents novel starch-based nanocomposites containing ZnS quantum dots capped with L-cysteine. The nanocomposites were prepared in form of gels and foils of potato starch with embedded spherical quantum dots sized 10-20 nm. They were characterized using photoluminescence, IR and UV spectra and TEM/SEM photographs. Pb²⁺ and Cu²⁺ ions decreased emission intensity of the photoluminescent spectral bands. The described quantum dots have been obtained using a simple, safe and low-cost method. Their properties make them alternative sensors for Pb²⁺ and Cu²⁺ ions that could be applied in biotechnology and food technology.

Keywords: starch, nanocomposites, heavy metals, nanosensors, quantum dots

INTRODUCTION

With their unique physical, chemical, biological and functional properties, inorganic nanocomposites have attracted special attention and some of them have found applications in various branches of industry, medicine, tissue engineering, pharmacy, optoelectronics, microelectronics, biological systems and as antimicrobial agents (Jeon and Baek, 2010; Kango *et al.*, 2013). In food technology, they serve to improve the functional properties of prepared products, monitor quality, decrease production costs and increase shelf life of ready-made food products (Ravichandran, 2010).

Recent years have seen a considerable development of nanosensors (Malik *et al.*, 2013). Novel nanosensors for food quality control can be designed using fullerenes,

carbon nanotubes and quantum dots (QDs). Such nanosensors and nanobiosensors are applicable in the monitoring of production processes (Berekaa, 2015; Bonilla *et al.*, 2016). They are also useful for pathogen and metal ion detection and quality assessment.

Currently, remarkable progress is being made in the development of robust and sensitive environmental sensors for various ions. Ion sensing can be performed with the use of QDs *via* analyte-induced changes in their photoluminescence (Jin *et al.*, 2005). These sensors could be qualified as (i) luminescence-based sensors mainly involving the photoluminescence and chemiluminescence processes and (ii) absorbance-based sensors detecting changes in spectral absorbance. Already back in 2002, CdS QDs capped with L-cysteine and thioglycerol were employed to detect zinc and copper in physiological buffer samples (Chen and Rosenzweig, 2002). QDs provided spectroscopic detection of metal ions including both transition (Zhang *et al.*, 2008) and heavy metals (Chen *et al.*, 2006; Mohamed *et al.*, 2007).

The sensors for biological systems should be environmentally-friendly and biodegradable. Generation of QDs in biopolymers may help in meeting such requirements. For that purpose, QDs have already been fixed to proteins (Vu *et al.*, 2005; Ornberg *et al.*, 2005; Gokarna *et al.*, 2008), amino acids (Rebilly *et al.*, 2008) and polysaccharides (Li and Han, 2008; Osaki *et al.*, 2004; Wang *et al.*, 2008).

Khachatryan *et al.* (2009; 2014; 2015; 2016) successfully prepared polysaccharide film matrices of starch, distarch phosphate, hyaluronic acid and maize amylopectin containing nanometer-sized semiconducting QDs.

*Corresponding author e-mail: rrgchacz@cyf-kr.edu.pl

Table 1. Volumes of added $\text{Pb}(\text{NO}_3)_2$ solution and water and final content of Pb^{2+} ions for the analysis

Sample number	0	1	2	3	4	5	6
$0.01000 \pm 0.0000015\text{M}$ $\text{Pb}(\text{NO}_3)_2$ (cm^3)	0	0.10	0.20	0.30	0.40	0.50	0.60
H_2O (cm^3)	1.00	0.90	0.80	0.70	0.60	0.50	0.40
Pb^{2+} final content (mol)	0	10^{-6}	2×10^{-6}	3×10^{-6}	4×10^{-6}	5×10^{-6}	6×10^{-6}

Table 2. Volumes of added $\text{Cu}(\text{NO}_3)_2$ solution and water and final content of Cu^{2+} ions for the analysis

Sample number	0	1	2	3	4	5	6
$0.01000 \pm 0.0000021\text{M}$ $\text{Cu}(\text{NO}_3)_2$ (cm^3)	0	0.10	0.20	0.30	0.40	0.50	0.60
H_2O (cm^3)	1.00	0.90	0.80	0.70	0.60	0.50	0.40
Cu^{2+} final content (mol)	0	10^{-6}	2×10^{-6}	3×10^{-6}	4×10^{-6}	5×10^{-6}	6×10^{-6}

Nanoparticles embedded in such matrices gained biodegradability, polyfunctionality, transparency and other interesting properties. The mentioned polysaccharides are biodegradable and readily undergo all physical, physico-chemical, chemical and enzymatic modifications which can extend the range of their applications.

In the project, we investigated a possibility of the formation of a novel biodegradable nanocomposite from cysteine, potato starch and ZnS quantum dots suitable as a sensor for selected heavy metal ions. The performance of that nanocomposite either as a gel or foil was checked against Pb^{2+} and Cu^{2+} ions. This paper describes a synthetic procedure for the preparation of starch/cysteine gel and film embedded with QDs nanoparticles. ZnS QDs were synthesized in an aqueous gel of starch plasticized with glycerol. Amino acids, especially these containing the thiol group, additionally stabilized the resulting nanoparticles and made them more biocompatible for biomedical applications. Foils emitting light on excitation with the UV light could readily be produced from the polysaccharide/QDs composites. The prepared materials were characterized by means of photoluminescence (PL), IR and UV spectra together with TEM/SEM photographs. The influence of the Pb^{2+} and Cu^{2+} ions on the optical properties of the developed QDs was also checked. The results suggest that the prepared nanocomposite could potentially serve as a suitable nanosensor for heavy metal ions.

MATERIAL AND METHODS

Sp/Cys-ZnS nanocomposites were prepared from gelatinized potato starch (Sp) of amylose: amylopectin ratio = 26 : 74; 12% moisture and 550 ppm phosphorus. It was purchased from Pepees SA, Łomża, Poland). Sp (4 g in 100 mL deionized water), glycerol (Aldrich, $\geq 99.5\%$) (2 g) and L-cysteine (Sigma, $\geq 98\%$) (0.5 g) were heated while continuously stirred until the solution was completely gelatinized (70°C for 30 min). The resulting gel was then treated with 0.4 mmol zinc acetate (Aldrich, 99.99%)

(0.4 mmol). After cooling to room temperature a stoichiometric amount of 0.1000 M aq. $\text{Na}_2\text{S} \cdot 9\text{H}_2\text{O}$ (Aldrich, $\geq 99.99\%$) solution was added.

For the photoluminescent analysis the gels (50.0000 g) were diluted with deionized water to the volume of 500 cm^3 followed by 15 min sonication in an ultrasonic bath at a temperature of 293 K. The prepared solutions (six 9.0 cm^3 portions) were poured into containers and treated with aqueous solutions containing different amounts of $\text{Pb}(\text{NO}_3)_2$ (Table 1) or $\text{Cu}(\text{NO}_3)_2$ (Table 2) (Aldrich, 99.99%). Then the volume of those solutions was increased to 10.0 cm^3 by the addition of deionized water.

Dry films in the form of elastic foils were prepared from the resulting gel poured onto a plastic plate by drying it at 50°C for 24 h.

The FTIR-ATR spectra of the composites were recorded in the range of $4000\text{--}700\text{ cm}^{-1}$ using a MATTSON 3000 FT-IR (Madison, Wisconsin, USA) spectrophotometer. That instrument was equipped with a 30SPEC 30 Degree Reflectance adapter fitted with the MIRacle ATR accessory from PIKE Technologies Inc., Madison, Wisconsin, USA.

Photoluminescence measurements for films and solutions were performed at room temperature using F7000 HITACHI spectrophotometer. The 270 nm wavelength was used for the excitation.

The UV-VIS absorption spectra were recorded with a Shimadzu 2101 scanning spectrophotometer in the range of 200-800 nm using 10 mL, 10 mm-thick quartz cells.

Analyses of sizes and morphologies of the as-prepared nanoparticles were studied using a high resolution JEOL 7550 scanning electron microscope equipped with TEM detector.

RESULTS AND DISCUSSION

ZnS QDs have been successfully prepared in an aqueous medium using potato starch as stabilizing agent and L-cysteine as capping reagent. As shown in the TEM image (Fig. 1), the prepared QDs provided spherical

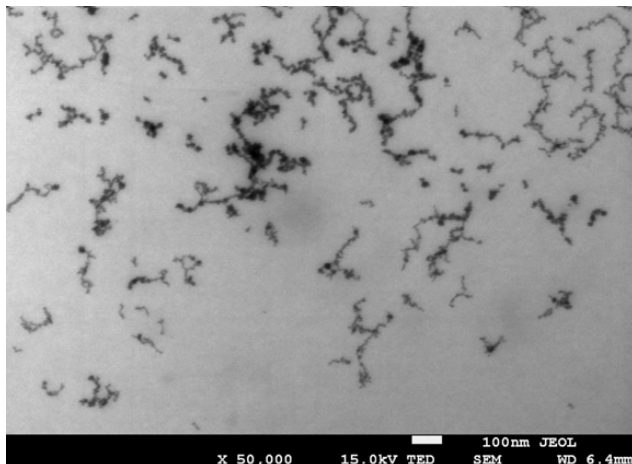


Fig. 1. TEM micrograph of Sp/Cys-ZnS taken at 50 000 magnification.

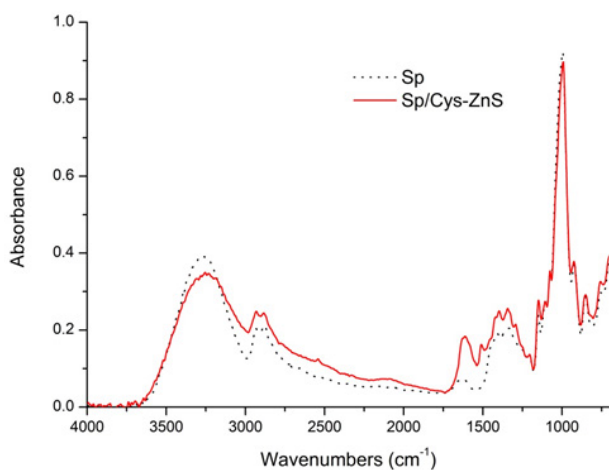


Fig. 2. FTIR spectra of Sp (black dotted line) and Sp/Cys-ZnS nanocomposite (red solid line).

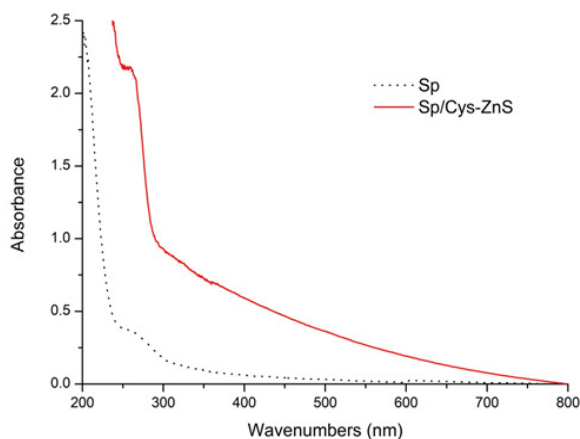


Fig. 3. UV-VIS spectra of Sp (black dotted line) and Sp/Cys-ZnS nanocomposite (red solid line).

granules of a narrow size distribution (10-20 nm) well- and fairly uniformly-dispersed in the medium. The FTIR spectra of Sp and Sp/Cys-ZnS composite films are shown in Fig. 2. The spectra showed bands at 1 150-950 cm^{-1} , with the band of 1 150 cm^{-1} corresponding to the asymmetric vibrations of the C-O-C bridging bonds where, at around 1100 cm^{-1} , asymmetric vibrations of the ring appeared and in the range of 1 080-960 cm^{-1} the stretching vibrations of the (C-O) bonds were visible. The spectra of all the samples presented bands at 2916-2936, 2855, 1405-1465 and at 1 245 cm^{-1} , which corresponded to the $-\text{CH}_2-$ group, as well as at 2880-2900 and 3 200 cm^{-1} , which corresponded to the C-H groups belonging to starch molecules (Warren *et al.*, 2016). Additionally, in the spectrum of the composite, the stretching vibration band of the carbonyl group of L-cysteine could be located at 1505-1 580 cm^{-1} . The shift of the C=O band from 1 635 to 1 505 cm^{-1} resulted from a resonance in the carboxylate group. Also, there was a weak peak at 2 540 cm^{-1} belonging to the cysteine thiol group stretching vibration. There was a strong resemblance of the spectra of both films. That resemblance provided evidence that the nanocomposite was a physical mixture of starch and Cys-ZnS.

The UV-VIS spectrum of Sp (Fig. 3) demonstrated a low absorption shoulder around 250 nm belonging likely to $n \rightarrow \pi^*$ transitions in the lone electron pairs in oxygen atoms. The spectrum of Sp with embedded QDs showed a strong absorption band around 280 nm followed by the long wavelength tail reaching its bottom in the spectrum of Sp/Cys-ZnS between 320-450 nm. The obtained spectra correspond with those presented in the literature. The fact that the UV-VIS absorption spectra are related to the size of the particles is well known (Rajabi *et al.*, 2013).

In order to validate the results of the metal ion sensor, PLS spectra of Sp/Cys-ZnS in the presence of the Cu^{2+} and Pb^{2+} ions were recorded at room temperature. The concentration of the tested aqueous solutions varied from 1×10^{-6} to 6×10^{-6} mol dm^{-3} . The PLS with excitation wavelength of 270 nm are shown in Fig. 4 (A) and (B), respectively. The spectra of Sp/Cys-ZnS showed the peak centred at 402 nm. The peak position of this blue emission did not significantly change with the increase in the Cu^{2+} and Pb^{2+} ion concentrations, but their intensity decreased with the increase in the concentration of the added metal ions forming S-shaped relationships specific for the applied metal ions.

Recent studies have reported that QDs with various capping molecules can serve as selective heavy metal sensors. Most of them present fluorescence quenching mechanisms including electron transfer process, ion binding interaction, inner filter effect and non radiative recombination pathway (Duan *et al.*, 2011). According to many papers, the addition of Cu^{2+} and Pb^{2+} significantly quenches the fluorescence intensity. This is caused by the interaction between the cation metal and QDs surface that may reduce

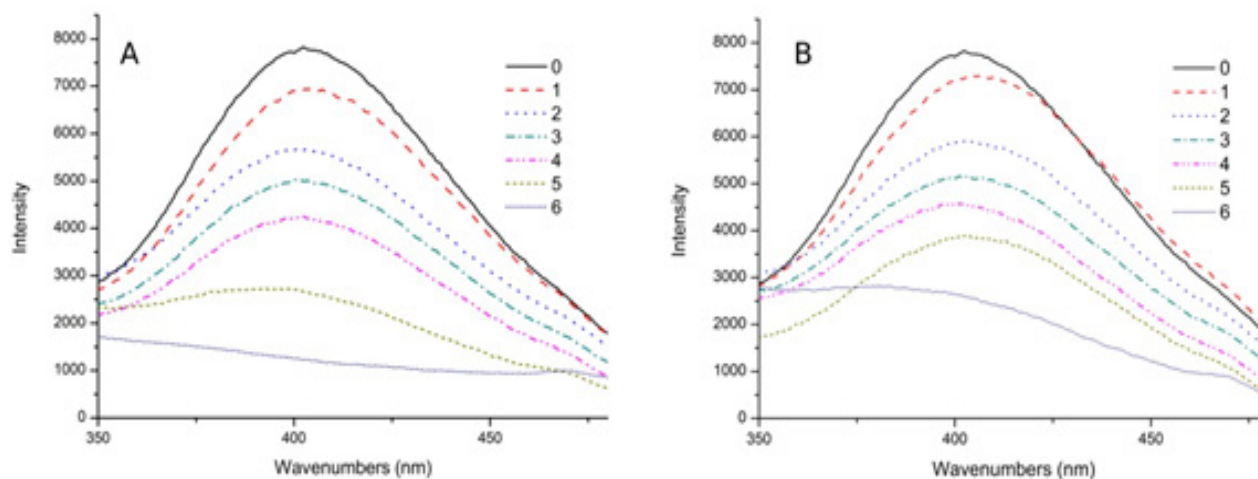


Fig. 4. Photoluminescence spectra of Sp/Cys-ZnS in presence of varying concentrations of (A) Cu^{2+} and (B) Pb^{2+} ions. Notation 0-6 corresponds to the number of the sample in Tables 1 (A) and 2 (B).

the electron-hole recombination. The effect depends on the concentration of added ions, which makes this system a sensitive and selective method for heavy metal sensing (Boonmee *et al.*, 2016). The emission intensities of Sp/Cys-ZnS nanocomposites in different molar concentrations of added Pb^{2+} and Cu^{2+} ions are presented in Fig. 5A. Both relationships are linear with a high determination coefficient, $R^2 = 0.985$ and 0.980 for Pb^{2+} and Cu^{2+} series, respectively.

For the series of 7 points, Eq. (1) for linear Intensity [a.u.] vs. ion concentration [mole] relationship:

$$y = a + bx, \quad (1)$$

where: a is an intercept and b is a slope in case of the Cu^{2+} cation provided solution $y = 7972.643 - 1.059E9x$ with determination coefficient $R^2 = 0.985$ and standard deviations $s = 6.147E7$. For the Pb^{2+} ions, the relationship $y = 7839.857 - 8.4461E8x$ with coefficient $R^2 = 0.980$ and standard deviations $s = 4.257E7$ was obtained. These

solutions and Fig. 5A demonstrate that the sensitivity of presented nanosensor depends on cations. Thus, it appeared more sensitive to Cu^{2+} ions than to Pb^{2+} ions.

The decrease in emission intensity in the presence of metal ions proves that the described nanocomposite may serve as an efficient, starch-based sensor for heavy metal ions.

The fluorescence quenching data for Pb^{2+} and Cu^{2+} ions were analyzed by the Stern-Volmer relationship (Eq. (2)), driven by the collision between the luminescent molecule and the quencher:

$$F_0/F = 1 + K_{SV}[Q], \quad (2)$$

where: F and F_0 are the luminescence intensities of the nanoparticles in the presence and absence of metal ion respectively, $[Q]$ is the copper or lead ion concentration, and K_{SV} is the Stern-Volmer quenching constant. The plots of F_0/F as a function of $[Q]$ for Pb^{2+} and Cu^{2+} ions are shown in Fig. 5B. These functions follow Eq. (3):

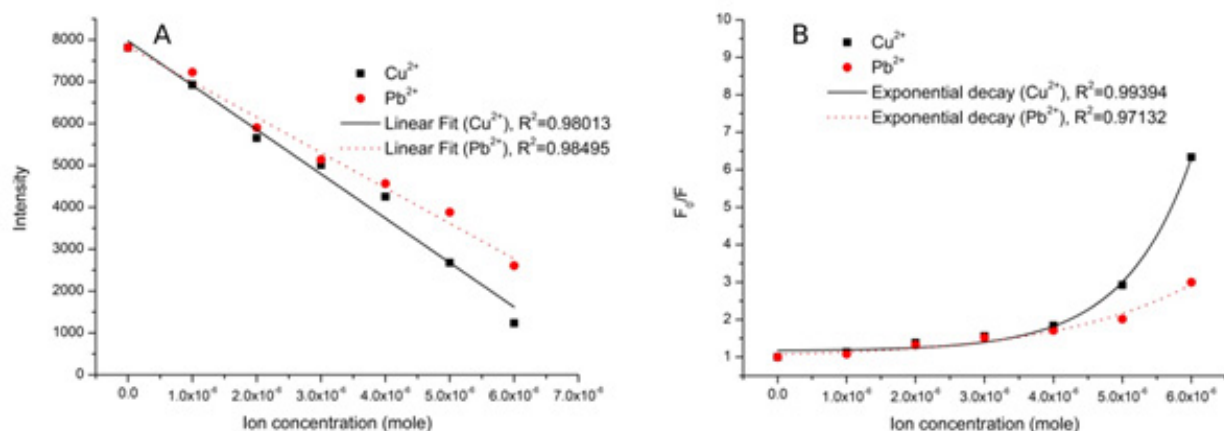


Fig. 5. Dependence of emission intensity (A) and F_0/F (B) and their linear fit (A) and exponential decay (B) of Sp/Cys-ZnS nanocomposite on the number of the molar concentration of the Pb^{2+} (red dotted line) and Cu^{2+} (black solid line) ions added (R^2 determination coefficient).

$$y = A_1 \exp(-x/t_1) + y_0, \quad (3)$$

where: t_1 and y_0 are the decay time and intercept, respectively. The solution of that equation for the Cu^{2+} ions was $y = 0.011\exp(x/9.712\text{E-}7) + 1.165$ with $R^2 = 0.994$ and $s = 0.087$, and for the Pb^{2+} ions the solution was $y = 0.097\exp(x/1.995\text{-E}6) + 0.972$ with $R^2 = 0.971$ and $s = 0.138$. In both cases these functions present an exponential decay. This dependence could be explained by the presence of both static and dynamic quenching (Koneswaran and Narayanaswamy, 2009).

Starch used in the synthesis is a well known heavy metal chelating agent, which forms complexes with Cu^{2+} and Pb^{2+} (Staroszczyk *et al.*, 2017). The composite formed elastic foils emitting blue light when excited with UV (365 nm) radiation (Fig. 6). When exposed to visible light the emission from that composite did not distinguish from the emission of starch. In the dark, visible light was emitted neither from the composite nor from starch.

The properties of the described foils make them a good potential material for intelligent food packaging to control food quality and safety (Fuertes *et al.*, 2016).

Therefore, potato starch, L-cysteine and ZnS quantum dots without any toxic stabilizers form a nanocomposite suitable as a nanosensor for heavy metal ions. It can be applied in the form of either gel or foil. Its sensitivity against the Cu^{2+} and Pb^{2+} cations has been proven in the ion concentration range of 1×10^{-6} to 6×10^{-6} mole dm^{-3} . The nanocomposites are physical mixtures of L-cysteine-ZnS complex in potato starch.

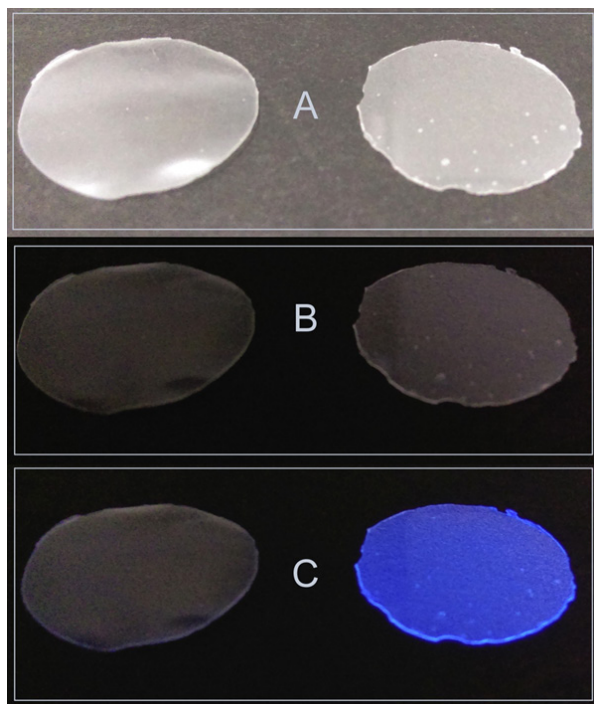


Fig. 6. Sp (left) and Sp/Cys-ZnS (right) foils illuminated with visible light (A), non-illuminated (B), and excited with the UV (365 nm) radiation (C).

CONCLUSIONS

1. The prepared ZnS quantum dots capped with L-cysteine reside within potato starch matrix forming spherical nanoparticles sized 10-20 nm, well dispersed in the composite.
2. Even small amounts of Pb^{2+} and Cu^{2+} ions (10-6 mol) caused a decrease in emission intensity of the photoluminescent spectral bands. This makes the potato starch – L-cysteine – ZnS composite a promising sensor for Pb^{2+} and Cu^{2+} ions.
3. Simple preparation without toxic stabilizers, makes the described nanosensors suitable for biotechnology and food technology.

Conflict of interest: The Authors declare they have no conflict of interest.

REFERENCES

- Berekaa M.M., 2015.** Nanotechnology in food industry; advances in food processing, packaging and food Safety. *Int. J. Current Microbiol. Applied Sci.*, 4, 345-357.
- Bonilla J.C., Bozkurt F., Ansari S., Sozer N., and Kokini J.L., 2016.** Applications of quantum dots in food science and biology. *Trends in Food Sci. Technol.*, 53, 75-89.
- Boonmee C., Noipa T., Tuntulani T., and Ngeontae W., 2016.** Cysteamine capped CdS quantum dots as a fluorescence sensor for the determination of copper ion exploiting fluorescence enhancement and long-wave spectral shifts. *Spectrochimica Acta Part A: Molecular and Biomolecular Spectroscopy*, 169, 161-168.
- Chen J., Gao Y., Xu Z., Wu G., Chen Y., and Zhu C., 2006.** A novel fluorescent array for mercury (II) ion in aqueous solution with functionalized cadmium selenide nanoclusters. *Analytica Chimica Acta*, 577, 77-84.
- Chen Y. and Rosenzweig Z., 2002.** Luminescent CdS quantum dots as selective ion probes. *Analytical Chemistry*, 74, 5132-5138.
- Duan J., Jiang X., Ni S., Yang M., and Zhan J., 2011.** Facile synthesis of N-acetyl-L-cysteine capped ZnS quantum dots as an eco-friendly fluorescence sensor for Hg^{2+} . *Talanta*, 85, 1738-1743.
- Fuertes G., Soto I., Carrasco R., Vargas M., Sabattin J., and Lagos C., 2016.** Intelligent packaging systems: sensors and nanosensors to monitor food quality and safety. *J. Sensors*, Article, ID 4046061. <https://doi.org/10.1155/2016/4046061>
- Gokarna A., Lee S.K., Hwang J.S., Cho Y.H., Lim Y.T., Chung B.H., and Lee M., 2008.** Fabrication of CdSe/ZnS quantum-dot-conjugated protein microarrays and nanoarrays. *J. Korean Physical Soc.*, 53, 3047.
- Jeon I.Y. and Baek J.B., 2010.** Nanocomposites derived from polymers and inorganic nanoparticles. *Materials*, 3, 3654-3674.
- Jin W.J., Fernández-Argüelles M.T., Costa-Fernández J.M., Pereiro R., and Sanz-Medel A., 2005.** Photoactivated luminescent CdSe quantum dots as sensitive cyanide probes in aqueous solutions. *Chemical Communications*, 7, 883-885.
- Kango S., Kalia S., Celli A., Njuguna J., Habibi Y., and Kumar R., 2013.** Surface modification of inorganic nanoparticles for development of organic-inorganic nanocomposites – A review. *Progress in Polymer Sci.*, 38, 1232-1261.

- Khachatryan G., Khachatryan K., Stobinski L., Tomasik P., Fiedorowicz M., and Lin H.M., 2009.** CdS and ZnS quantum dots embedded in hyaluronic acid films. *J. Alloys Compounds*, 481, 402-406.
- Khachatryan K., Khachatryan G., and Fiedorowicz M., 2015.** Synthesis of ZnS, CdS and Core-Shell Mixed CdS/ZnS, ZnS/CdS Nanocrystals in Tapioca Starch Matrix. *J. Materials Sci. Chemical Eng.*, 3, 30.
- Khachatryan K., Khachatryan G., Fiedorowicz M., and Tomasik P., 2014.** Formation and properties of selected quantum dots in maize amylopectin matrix. *J. Alloys Compounds*, 607, 39-43.
- Khachatryan K., Khachatryan G., and Fiedorowicz M., 2016.** Distarch Phosphate as a Matrix for the Generation of Quantum Dots. *Polymers Polymer Composites*, 24, 403.
- Koneswaran M. and Narayanaswamy R., 2009.** L-Cysteine-capped ZnS quantum dots based fluorescence sensor for Cu²⁺ ion. *Sensors and Actuators B: Chemical*, 139, 104-109.
- Li H. and Han C., 2008.** Sonochemical synthesis of cyclodextrin-coated quantum dots for optical detection of pollutant phenols in water. *Chemistry of Materials*, 20, 6053-6059.
- Malik P., Gulia S., and Kakkar R., 2013.** Quantum dots for diagnosis of cancers. *Advanced Materials Letters*, 4, 811-822.
- Mohamed Ali E., Zheng Y., Yu H.H., Ying J.Y., 2007.** Ultrasensitive Pb²⁺ detection by glutathione-capped quantum dots. *Analytical Chemistry*, 79, 9452-9458.
- Ornberg R.L., Harper T.F., and Liu H., 2005.** Western blot analysis with quantum dot fluorescence technology: a sensitive and quantitative method for multiplexed proteomics. *Nature Methods*, 2, 79.
- Osaki F., Kanamori T., Sando S., Sera T., and Aoyama Y., 2004.** A quantum dot conjugated sugar ball and its cellular uptake. On the size effects of endocytosis in the subviral region. *J. Am. Chemical Soc.*, 126, 6520-6521.
- Rajabi H. R., Shamsipur M., Khosravi A.A., Khani O., and Yousefi M.H., 2013.** Selective spectrofluorimetric determination of sulfide ion using manganese doped ZnS quantum dots as luminescent probe. *Spectrochimica Acta Part A: Molecular and Biomolecular Spectroscopy*, 107, 256-262.
- Ravichandran R., 2010.** Nanotechnology applications in food and food processing: innovative green approaches, opportunities and uncertainties for global market. *Int. J. Green Nanotechnology: Physics and Chemistry*, 1, 72-96.
- Rebilly J.N., Gardner P.W., Darling G.R., Bacsá J., and Rosseinsky M.J., 2008.** Chiral II–VI semiconductor nanostructure superlattices based on an amino acid ligand. *Inorganic Chemistry*, 47, 9390-9399.
- Staroszczyk H., Ciesielski W., and Tomasik P., 2017.** Starch – metal complexes and metal compounds. *J. Sci. Food Agric.*, <https://doi.org/10.1002/jsfa.8820>
- Vu T.Q., Maddipati R., Blute T.A., Nehilla B.J., Nusblat L., Desai T.A., 2005.** Peptide-conjugated quantum dots activate neuronal receptors and initiate downstream signalling of neurite growth. *Nano Letters*, 5, 603-607.
- Wang C.H., Hsu Y.S., and Peng C.A., 2008.** Quantum dots encapsulated with amphiphilic alginate as bioprobe for fast screening anti-dengue virus agents. *Biosensors Bioelectronics*, 24, 1012-1019.
- Warren F.J., Gidley M.J., and Flanagan B.M., 2016.** Infrared spectroscopy as a tool to characterise starch ordered structure – a joint FTIR-ATR, NMR, XRD and DSC study. *Carbohydrate Polymers*, 139, 35-42.
- Zhang Y., Li Y., Dong L., Li J., He W., Chen X., and Hu Z., 2008.** Investigation of the interaction between naringin and human serum albumin. *J. Molecular Structure*, 875, 1-8.